

Luminescence chronology of “Old Red Sand” in Jinjiang and its implications for optical dating of sediments in South China

ZHANG JiaFu^{1†}, YUAN BaoYin² & ZHOU LiPing¹

¹Laboratory for Earth Surface Processes, Department of Geography, Peking University, Beijing 100871, China;

²Institute of Geology and Geophysics, Chinese Academy of Sciences, Beijing 100029, China

A weathered deposit in South China is widespread on the coastal areas of Fujian and Guangdong provinces, China. This deposit consists of slightly cemented, medium- to fine-grained sands, and is characterized by its colors of red, brown red, light reddish brown or dark yellowish orange, and is usually called “Old Red Sand”. The uncertainty in its formation age has been a major obstacle to the study of this type of deposit. In this paper, optically stimulated luminescence (OSL) techniques were used to date the “Old Red Sand” sediments from Jinjiang, Fujian Province, China. The effect of the geochemical behavior of uranium and thorium in sediment during chemical weathering on estimation of annual dose was investigated. The results show that the change in annual dose due to weathering poses a major problem for the optical dating of such weathered sediments. The optical dating of these weathered deposits will produce erroneous ages if average annual dose during burial cannot be correctly estimated. For the profiles studied, the OSL dates obtained on samples from the upper part do not represent the burial age of the samples. It is highly likely that they are underestimated due mainly to the accumulated radioactive elements as a result of chemical weathering. It is concluded that changes in annual dose due to chemical weathering must be considered when dating similar sediments in South China. With a detailed analysis of the OSL dating results, the chronology of the marine terraces in this area was suggested. The lowest terrace was formed at ~3.5 ka and the second terrace was dated to ~74 ka. The age of the highest terrace may not be established accurately, but is inferred to be older than the apparent OSL date of ~77 ka and so is the Paleolithic artifacts from it.

“Old Red Sand”, optical dating, annual dose, chemical weathering, marine terrace, Jinjiang

A Quaternary deposit, usually called “Old Red Sand”, in South China is widespread on the coastal areas of Fujian and Guangdong provinces, South China. This kind of deposit consists of slightly cemented, medium- to fine-grained sands, and is characterized by its colors of red (10R4/8), brown red (2.5YR4/8), light reddish brown (5YR5/8), dark yellowish orange (5YR/5/8). It is distributed in the areas with modern coastal dunes along the coast of South China and has suffered different degrees of chemical weathering. This sand sediment, in the form of single or multiple sand embankments, has continuous distribution along the coastal plains, or on hillslopes

near the coastline^[1,2]. The sedimentary characteristics and the genesis of the “Old Red Sand” sediment have been widely investigated by Chinese scientists^[1–7]. Its formation age has attracted the considerable attention of geologists and geomorphologists, but has not been well dated. Most of the dates of the sediment reported were obtained by using radiocarbon dating for organic materials from sediments underlying or overlying the “Old

Received May 9, 2007; accepted October 18, 2007

doi: 10.1007/s11434-008-0001-6

†Corresponding author (email: jfzhang@pku.edu.cn)

Supported by the National Natural Science Foundation of China (Grant Nos. 40471010 and 49925307)

Red Sand” sediment, or thermoluminescence (TL) dating and ESR dating for the sediment^[5,7–9]. The ages reported range from 9 to 70 ka, concentrating on 10–30 ka, many of which were obtained by using TL techniques.

Recently developed optically stimulated luminescence (OSL) dating techniques for sediments have many advantages over TL dating techniques^[10–12]. One of them is that OSL signals are more effectively zeroed than TL signals^[13]. The OSL “clock” of sediments is very quickly zeroed when sediments are exposed to daylight. After deposition, the clock starts to tick again due to the radioactivity in the sedimentary environment. The optical ages of sediments are the time since its last exposure to daylight. Therefore, OSL techniques are a direct dating method for sediments. Luminescence dating materials are detrital minerals: quartz and feldspar grains, and so it can be applied to almost all types of Quaternary sediments^[14]. Recently, precision and accuracy in optical ages are greatly improved due to the development of dating techniques^[15,16]. Coastal dune sand and beach sand, either young sample (6 ± 2 a)^[17] or old sample (141 ± 7 ka)^[18], have been dated using the optical techniques. From an optically bleachable point of view, the “Old Red Sand” sediment originated from wind-blown^[1] or coastal sediments^[19] at deposition along the coastlines of Fujian and Guangdong provinces, China, should be datable material for optical techniques. However, strong weathering in the area may lead to changes in chemical composition of the sediments which would have some effect on the optical dating results.

The “Old Red Sand” sediment is broadly distributed along the coast of Jinjiang, Fujian Province. It has been widely investigated by many workers^[6–8, 20]. The Jinjiang area is also characterized by ancient submerged forest^[21], paleoearthquake^[22] and Paleolithic sites¹⁾, and it has been approved to be the Shenhuanwan National Geological Park in Jinjiang, Fujian Province. In this paper, the effect of weathering on optical dating is investigated on “Old Red Sand” samples from the Xiangzhi and Shenhu sections located at marine terraces in this area. In particular, the effect of the re-mobilization and migration of uranium and thorium in sediments due to weathering were discussed.

1 Geological background and sampling

The coastal area of Jinjiang is well known for the “Old Red Sand” sediment. Based on elevation and sedimentary features, three marine terraces in this area were identified. The elevations above sea level (a.s.l.) of the terraces are similar to those in the southeastern coastal area of Korean Peninsula^[23,24]. The lowest terrace (T1) is located at the coastal area close to the modern coastline. Its elevation is generally 3–5 m a.s.l., up to 10 m a.s.l. in some places. The terrace deposits, consisting mainly of grayish yellow clayey fine sand, are coastal sediments. Three OSL samples (JJ-10, JJ-11 and JJ-12) were taken from the Jintiancun (JT) and Shizhencun (SZ) sections in farmland on this terrace. In order to assess the degree of bleaching of coastal sediments, two modern dune sand samples (JJ-D1 and JJ-D2) and two modern beach sand samples (JJ-B1 and JJ-B2) were collected from the coast of the Shenhuanwan (SHW) Bay in Jinjiang (Figures 1 and 2).

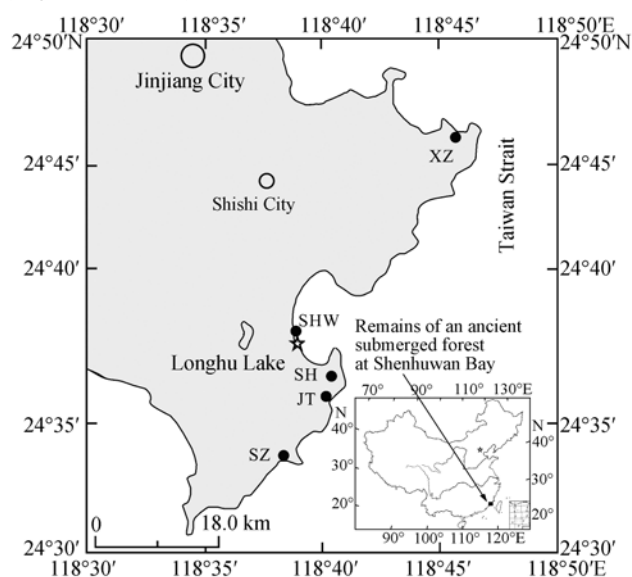


Figure 1 Location map showing the study area and the section sites for OSL sampling. XZ: Xiangzhi section, SHW: Shenhuanwan section, SH: Shenhu section, JT: Jintiancun section, SZ: Shizhencun section.

The second terrace (T2) varies from 20 to 30 m a.s.l. The terrace deposits can be represented by the sediments in the Xiangzhi (XZ) section ($24^{\circ}46'13.0''\text{N}$, $118^{\circ}45'43.9''\text{E}$) (Figures 1 and 2). The color of the sediments changes from dark reddish brown at the top to

1) Yuan B Y, Ceng R S, Li R Q, et al. A report of the Shenhuanwan National Geological Park in Jinjiang, Fujian Province. Institute of Geology and Geophysics, Chinese Academy of Sciences, 2003

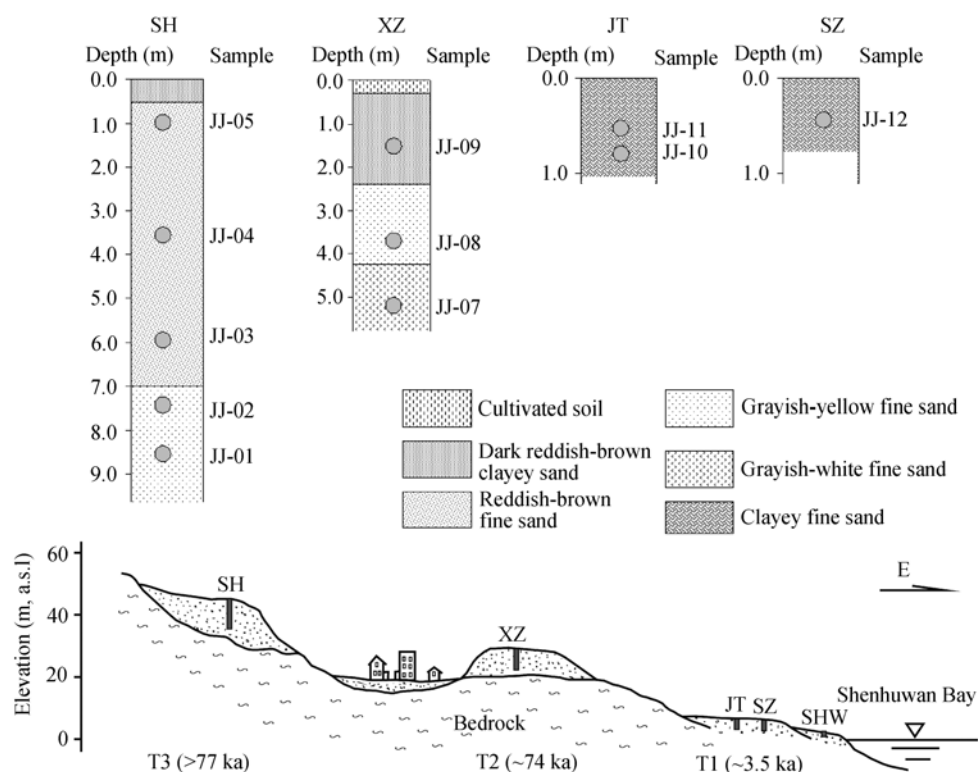


Figure 2 Sketch map showing the three marine terraces in Jinjiang, Fujian Province, China, and the sections for OSL sampling. XZ, Xiangzhi section; SHW, Shenhuan section; SH, Shenhu section; JT, Jintiancun section; SZ, Shizhencun section.

grayish white at the bottom of the section, indicating that the degree of weathering of the sediments is lessened from top to bottom. According to sediment color, the section is divided into four units, the color between units is gradual (Figure 2). The top unit is 0.3 m thick cultivated soil, and underneath is a soil of 2.1 m thick dark reddish-brown sand overlying on a 1.8 m thick grayish-yellow middle-fine sand layer. At the bottom is 1.6 m thick very well-sorted grayish-white fine quartz sand unit which appears to have hardly been affected by weathering. Three OSL samples (JJ-07, JJ-08 and JJ-09) were collected from this section (Figures 1 and 2).

The highest terrace (T3) has an altitude of 40–50 m a.s.l and a 10-m section is found at Shenhu (SH) ($24^{\circ}36'53.6''\text{N}$, $118^{\circ}40'25.8''\text{E}$) (Figures 1, 2). Based on sediment color, the section is divided into three units. At the top of the section, there is laterite consisting of 0.5-m-thick dark reddish-brown sandy clay. In the middle part of the section is 6.5-m-reddish-brown fine to medium sand. The sediment at the bottom is grayish-yellow fine sand believed to be ancient dune sand (see footnote 1) on page 592). The intensity of weathering decreases from the top to bottom of the section. A vein quartz pebble with percussion bulb was identified

as a core with hammer percussion by archaeologists (see footnote 1) on page 592). In this section, a total of five OSL samples (JJ-01, JJ-02, JJ-03, JJ-04 and JJ-05) were collected, and samples JJ-01 and JJ-02 are ancient dune sand (Figure 2).

All the samples for optical dating were collected by hammering metal tubes horizontally into freshly cleaned vertical sections. Once removed, the tubes were immediately sealed tightly at both ends with tinfoil and tapes to ensure that the samples had retained their natural water contents.

2 Experimental details

2.1 Annual dose

The radioactivity of sediment is mainly from the radiation decay of ^{235}U , ^{238}U , ^{232}Th and their daughter nuclides, and ^{40}K in the sediment. The radiation dose absorbed by mineral grains during burial depends primarily on the contents of radionuclides in sediment and dated grains themselves. The U, Th and K contents of these samples were determined using Neutron Activation Analysis in China Institute of Atomic Energy. The cosmic ray contribution to annual dose was calculated

using the function suggested by Prescott and Hutton^[25]. The water content (the ratio of the weight of water to the weight of the dry sample) was determined by weighing sample before and after drying. Uncertainties in water content were assigned to 10% for all samples. Finally, the elemental concentrations were converted into annual dose according to Aitken^[12].

2.2 Equivalent dose

Under subdued red light in the laboratory's dark room, materials at both ends of the sample tubes were removed. The remaining samples (interior parts) were then treated with H₂O₂ to remove organic material, and then dilute HCl to dissolve carbonates followed by washing with distilled water. The samples were then dried, and sieved to obtain 150–250 μm grains for equivalent dose (*D_e*) measurements. They were etched by 40% HF to remove feldspar contaminants in order to obtain pure quartz. The etching duration depends on the residual IRSL signals of the treated samples. Finally, the quartz extracts were mounted on 0.97 cm diameter aluminum discs using silicon oil.

The equivalent doses of the samples were estimated using the single-aliquot regenerative-dose (SAR) method^[15,26]. The advantage of the SAR protocol is that sensitivity changes during the measurement procedure can be corrected by using a signal induced by a test dose. Regenerative beta doses including a zero dose and a repeated dose were employed, and the corresponding sensitivity-corrected OSL signals (regenerated OSL signal divided by the subsequent test-dose OSL signal) were used to construct growth curves (Figure 3). The value of *D_e* (single-aliquot *D_e*) was estimated by interpolating sensitivity-corrected natural OSL onto a growth

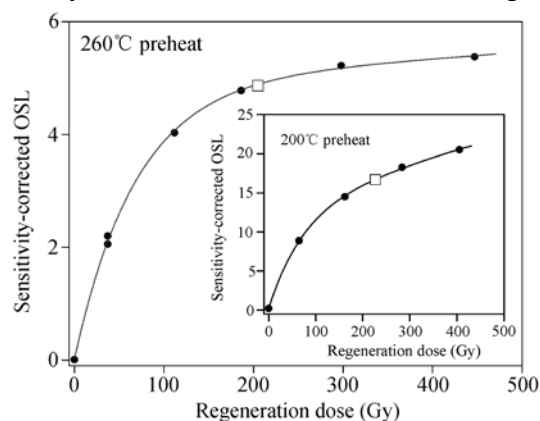


Figure 3 Growth curves for sample JJ-07 obtained by the SAR method (see text). Open squares represents natural OSL signals and solid circles refer to regenerative signals.

curve. All OSL signals were measured for 40 s at a sample temperature of 125°C.

All luminescence measurements, beta irradiation and preheat treatments were carried out on a TL/OSL reader (Risø-TL/OSL-15) equipped with a ⁹⁰Sr/⁹⁰Y beta source. Blue light (470±30 nm) LED stimulation (90% of 50 mW/cm² full power) was used for OSL measurements. Luminescence was detected by an EMI 9235QA photomultiplier tube with three 2.5 mm Hoya U-340 filters (290–370 nm) in front of it.

3 Results and discussion

3.1 Annual dose

The uranium, thorium and potassium contents of the samples and their calculated effect annual doses are listed in Table 1 and displayed in Figure 4. For the dune sample (JJ-D2), its U and Th contents (0.91±0.05 and 5.66±0.18 μg/g, respectively) and annual dose (1.09±0.03 Gy/ka) are similar to those of coastal and inland dune samples^[17,27–31] from other areas, but are lower compared to the other samples from Jinjiang. The U and Th contents and the annual doses of the samples (JJ-10, JJ-11 and JJ-12) from T1 are much higher than those of the coastal dune sample (JJ-D2). The U and Th contents of the samples in the Xiangzhi and Shenhu sections decrease with depth. The annual dose of the samples from the Shenhu section is reduced from 3.25 Gy/ka at the top to 1.42 Gy/ka at the bottom of the section (Table 1; Figure 4).

The Xiangzhi and Shenhu sections are “typical” weathering profiles for the “Old Red Sand” sediment in the coastal areas of South China, the intensity of weathering decreases with depth. The tendency to decrease in weathering from the top to bottom of the sections can be observed in the following aspects: (1) clay mineral contents and the degree of cementation of the sediment are reduced, and the clay contents are 6.31%, 3.15% and 1.33% at the depths of 1.3, 3.6 and 4.6 m in the Xiangzhi section, respectively^[6]. The clay consists mainly of kaolinite formed during chemical weathering^[4]. (2) SiO₂ content increases, but Al₂O₃, Fe₂O₃ and FeO contents decrease^[1], resulting from element migration caused by chemical weathering^[32,33]. (3) Sediment color changes from dark reddish brown to grayish white, reflecting the degree of oxidation of the “Old Red Sand” sediment^[3]. Based on the above criteria, it is considered

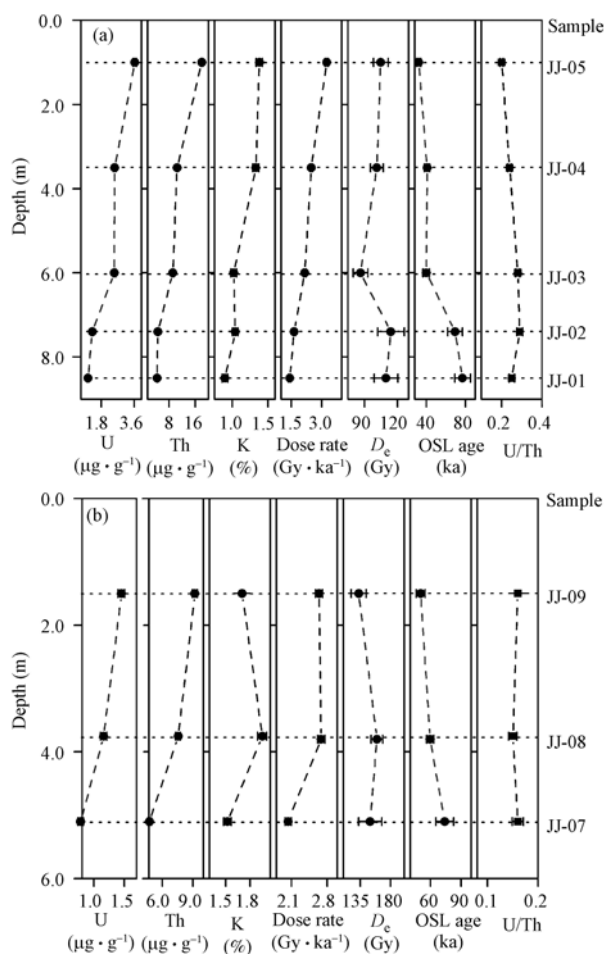


Figure 4 U, Th and K contents, annual dose, D_e , OSL age and U/Th ratio for the samples in the Shenhu (a) and Xiangzhi (b) sections.

that the degree of weathering of the sediments in the Shenhu section in T3 is higher than that of the Xiangzhi section in T2.

The decrease in U and Th contents with increasing depth in the Xiangzhi and Shenhu sections results from element migration and enrichment caused by chemical weathering. This can be explained by the geochemical behaviors of uranium and thorium in sediments during weathering^[34–43]. For example, chemical weathering causes U and Th in rocks to be redistributed in weathering products^[34,35], and be enriched during later pedogenesis^[36–38]. In these two sections, the bottom samples (JJ-01, JJ-02 and JJ-07) are less affected by weathering, their U and Th contents are very similar to those of the modern dune sand (sample JJ-D2), suggesting that their U and Th contents have been constant since deposition. For the upper samples, the increase in U and Th contents is due to migration or loss of other elements such as Ca and Si, resulting in a relative enrichment of

U and Th in the upper samples. On the other hand, for the top samples, their U contents are also affected by long-term fertilizer applications, which results in accumulation of uranium^[44].

Uranium migrates preferentially, and thorium is relatively immobile during weathering^[33,45]. This suggests that the U/Th ratios would be reduced when the degree of weathering increases^[46]. The U/Th ratios of the samples in the Xiangzhi and Shenhu sections remain constant from top to bottom. The ratios of the samples from the Shenhu section in T3 are much higher than the ratios of the samples from the sections in T1 and T2. The latter are similar to the ratio of the modern coastal dune sample (JJ-D2). This suggests that weathering did not lead to loss of U in the “Old Red Sand” sediment in this area. This may imply that U-containing minerals in the “Old Red Sand” sediment are derived from the weathering-resistant minerals in the weathered granite while the weathering of the marine beach deposits was dominated by the process of desilication coupled with Al-enrichment.

As shown in Table 1 and Figure 4, the K content decreases downwards in the Shenhu section but is higher in the Xiangzhi section on T2, varying in the range of 1.52%–1.92%. The causes of such K distribution and its effect on the calculation of the annual dose are unclear and require further investigations.

The above discussions demonstrate that chemical weathering causes changes in chemical composition and a relative enrichment of U and Th in weathered sediments. The change in composition depends on the degree of weathering. Therefore, the annual dose, calculated from the contents of radioactive elements determined presently, only represents the recent annual dose of the sample, not the average annual dose during burial. In this case, assuming U- and Th decay series in radioactive equilibrium, the calculated annual dose would be overestimated for age calculation due to an enrichment of U and Th in weathered sediments. Nevertheless, if the samples at the bottom of the Xiangzhi and Shenhu sections are relatively little affected by chemical weathering. Their annual doses should be close to the average annual doses of the dated samples during burial.

3.2 D_e measurements

To determine appropriate preheat conditions for D_e estimation, preheating plateau tests were carried out on sample JJ-05 in the temperature range of 160–260°C.

Table 1 Results of optical dating

Lab No.	Filed No.	Depth (m)	U ($\mu\text{g}\cdot\text{g}^{-1}$)	Th ($\mu\text{g}\cdot\text{g}^{-1}$)	U/Th ratio	K (%)	Cosmic dose rate ($\text{Gy}\cdot\text{ka}^{-1}$)	Water content (%)	Total dose rate ($\text{Gy}\cdot\text{ka}^{-1}$)	D_e (Gy)	Age (ka)
Shenhuwan (SHW) modern beach											
PKU-L282	JJ-B1	0.1	nd	nd		nd		nd		0.027±0.022	
PKU-L283	JJ-B2	0.1	nd	nd		nd		nd		0.004±0.003	
Shenhuwan (SHW) modern coastal dune											
PKU-L284	JJ-D1	1.0	nd	nd		nd		nd		0.09±0.02	0.08±0.02 ^{a)}
PKU-L285	JJ-D2	3.5	0.91±0.05	5.66±0.18	0.16±0.01	0.35±0.02	0.19	3.7	1.09±0.03	0.20±0.05	0.18±0.05
The first marine terrace (T1) in Jintiancun											
PKU-L295	JJ-10	0.8	2.12±0.07	11.80±0.28	0.18±0.01	1.23±0.04	0.19	3.1	2.60±0.06	9.10±1.90	3.5±0.7
PKU-L296	JJ-11	0.5	2.10±0.06	11.40±0.26	0.18±0.01	1.02±0.04	0.19	1.6	2.41±0.06	0.16±0.04	0.07±0.02
The first marine terrace (T1) in Shizhencun											
PKU-L297	JJ-12	0.4	1.70±0.06	9.36±0.25	0.18±0.01	1.33±0.04	0.19	14.9	2.16±0.06	0.70±0.03	0.32±0.02
The second marine terrace (T2) in Xiangzhi (SZ)											
PKU-L292	JJ-07	5.1	0.78±0.04	4.77±0.17	0.16±0.01	1.52±0.05	0.09	1.7	2.03±0.06	149.5±17.3	73.8±8.8
PKU-L293	JJ-08	3.8	1.16±0.05	7.55±0.22	0.15±0.01	1.95±0.05	0.11	3.2	2.68±0.07	159.60±8.50	59.5±3.5
PKU-L294	JJ-09	1.5	1.45±0.06	9.17±0.24	0.16±0.01	1.70±0.05	0.16	4.4	2.64±0.07	132.60±11.20	50.2±4.4
The third marine terrace (T3) in Shenhu (SH)											
PKU-L286	JJ-01	8.5	1.08±0.04	4.38±0.17	0.20±0.01	0.90±0.04	0.06	3.7	1.42±0.05	109.50±10.70	77.0±8.0
PKU-L287	JJ-02	7.4	1.32±0.05	4.56±0.17	0.24±0.01	1.04±0.04	0.07	2.8	1.64±0.05	114.00±12.00	69.3±7.6
PKU-L288	JJ-03	6.0	2.52±0.06	9.15±0.25	0.28±0.01	1.02±0.04	0.07	4.4	2.17±0.06	86.40±6.60	39.8±3.2
PKU-L289	JJ-04	3.5	2.53±0.07	10.50±0.26	0.29±0.01	1.33±0.04	0.11	8	2.49±0.06	101.20±6.00	40.7±2.6
PKU-L290	JJ-05	1.0	3.63±0.09	18.00±0.36	0.25±0.01	1.38±0.04	0.17	9.4	3.25±0.08	104.80±6.70	32.2±2.2

a) Calculated with the dose rate of sample JJ-D2.

For the other samples, their D_e s were determined using the preheats of 200°C and 260°C for 10 s with a cutheat of 160°C. The results are shown in Figure 5. It can be seen that D_e is independent of preheat temperature at least in the range of 200–260°C except for sample JJ-07. Figure 5 also shows the scatter of the D_e values obtained using a preheat of 260°C is larger than that using a preheat of 200°C. In addition, the growth curves obtained using a preheat of 260°C for some aliquots exhibit a saturation trend compared with those obtained using a preheat of 200°C (Figure 3). This phenomenon requires further investigations.

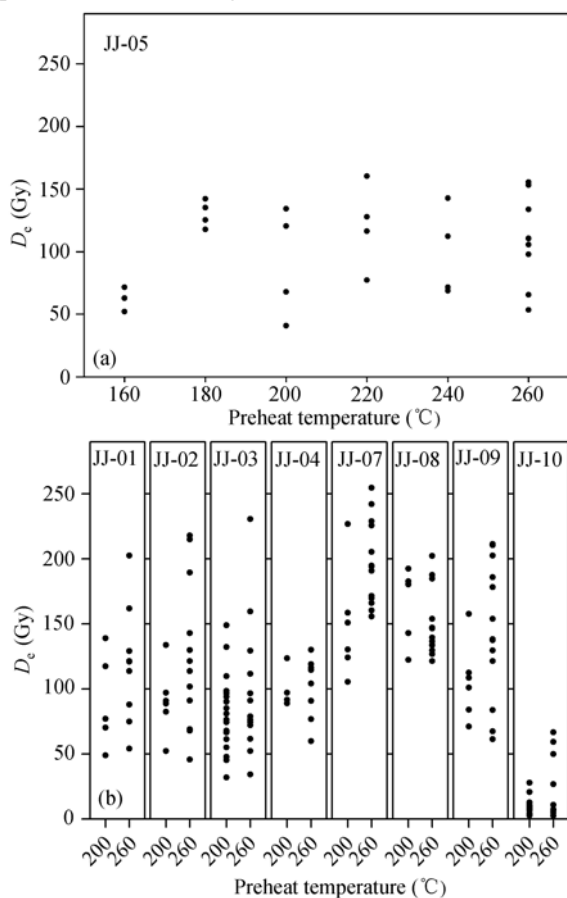


Figure 5 Plot of equivalent dose versus preheat temperature.

In order to further test the suitability of the preheat conditions determined by the above preheat plateau tests, dose recovery tests^[47,48] were carried out on sample JJ-05. The natural OSL signal from an aliquot was completely bleached out by exposing the aliquot to the blue light in the OSL reader at room temperature. It was then irradiated with a beta dose (given dose). The irradiated

aliquot was measured using the SAR method, and a “measured dose” was obtained. The ratios of “measured dose” to “given dose” are plotted as a function of preheat temperatures (Figure 6). It demonstrates that the “measured doses” are in agreement with the given dose within error limits in the preheating plateau. This suggests that the D_e s obtained for this sample using the preheat conditions determined by the above preheating plateau tests are reliable.

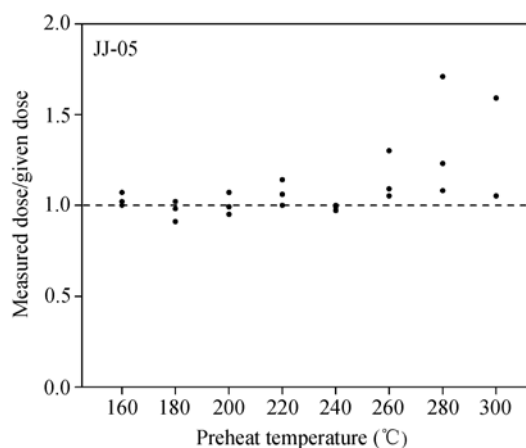


Figure 6 Results of dose recovery tests for sample JJ-05.

The average D_e values for these samples are listed in Table 1. The distribution of D_e values for sample JJ-03 is displayed in Figure 7, which indicates that these samples were well bleached at the time of deposition. On the other hand, for old samples such as JJ-03, the uncertainty in zeroing of the OSL signals is relatively insignificant for age calculation^[47,48]. The large scatter in D_e is most likely to be due to heterogeneous of radionuclides in the sediments. For comparison, Figure 7 also gives the results of the D_e values of the modern dune sample (JJ-D1). The average D_e for this modern sample is 0.09 ± 0.02 Gy. In addition, the average D_e values for the two modern beach sand samples (JJ-B1 and JJ-B2) are 0.03 ± 0.02 and 0.004 ± 0.003 Gy, respectively. Therefore, it is inferred that the residual signals of these “Old Red Sand” samples at deposition are negligible for age calculation. Hence, their optical ages cannot be overestimated due to their residual signals at deposition.

3.3 Optical ages

The optical ages are obtained by dividing average D_e values by annual dose using Grün’s program¹⁾. The calculated results are listed in Table 1. The optical ages of

1) Grün R. Age.exe. Computer program for the calculation of luminescence dates. Unpublished Computer RSES, Canberra. 2000

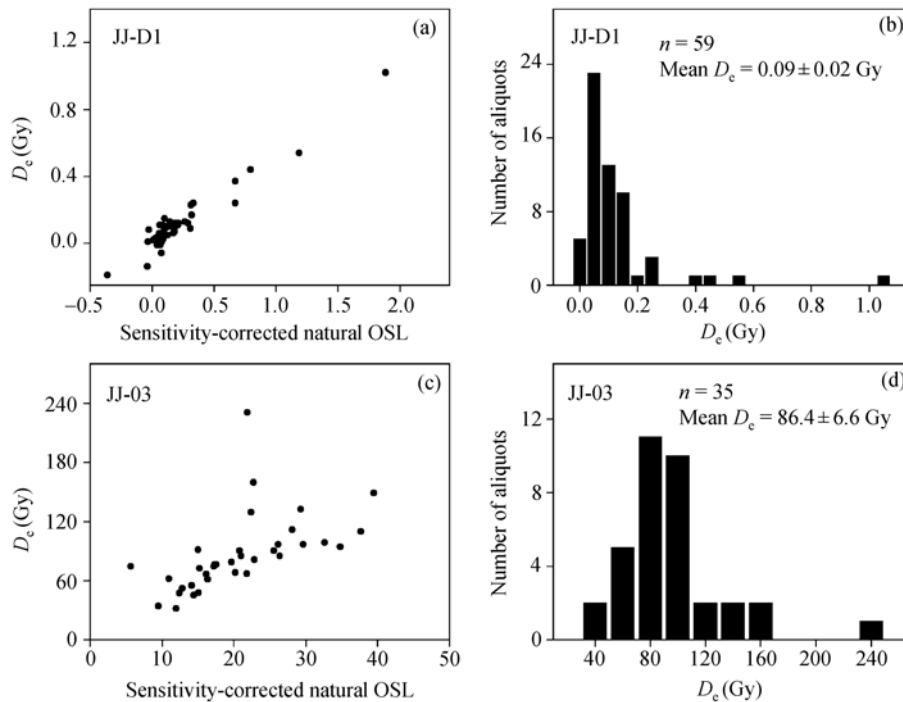


Figure 7 Distribution of equivalent dose values for samples JJ-03 and JJ-D1. The negative values for sample JJ-D1 result from laboratory measurement errors.

the two modern coastal dune sand samples are 0.18 ± 0.05 and 0.08 ± 0.02 ka, respectively. The ages of samples JJ-10, JJ-11 and JJ-12 from T1 are 3.5 ± 0.7 , 0.07 ± 0.02 and 0.32 ± 0.02 ka. Samples JJ-11 and JJ-12 taken from near the ground surface of the section located at the cultivated soil might be affected by human activities. Samples JJ-07, JJ-08 and JJ-09 from the Xiangzhi section in T2 were dated to 73.8 ± 8.8 , 59.5 ± 3.5 and 50.2 ± 4.4 ka, respectively. The optical ages of samples JJ-01, JJ-02, JJ-03, JJ-04 and JJ-05 from the Shenhu section in T3 are 77.0 ± 8.0 , 69.3 ± 7.6 , 39.8 ± 3.2 , 40.7 ± 2.6 and 32.2 ± 2.2 ka, respectively. The optical ages of these samples are all in stratigraphic order. However, the difference in age among the samples from different depths of the Xiangzhi and Shenhu sections may result from the erroneous estimation of annual dose, these ages are not their true burial ages.

The annual doses of the samples from the Xiangzhi and Shenhu sections decrease with increasing depth (Figure 4). The D_e values of the samples from the upper and the lower parts of the sections are very similar. This may suggest that the change in age with depth is caused by the different annual doses of these samples. As discussed above, chemical weathering results in a relative enrichment of U and Th in weathering products, and therefore the annual doses of the weathered samples

calculated from the contents of radioisotopes determined presently are larger than their average annual doses during burial. The overestimation of the annual doses of these relatively strongly weathered samples at the upper part of the sections results in their underestimated ages. By comparison, if the samples at the bottom of the sections are little affected by weathering, then the radioactive elements should remain largely unchanged, and hence the calculated annual dose should represent the average dose during burial. The similarity in annual dose between the dune sand samples (JJ-01 and JJ-02) at the bottom of the Shenhu section and the modern coastal dune sand sample (JJ-D1) may suggest such a case. Therefore, the optical ages of these relatively less weathered samples should be closest to their true burial ages.

3.4 Ages of marine terraces and Paleolithic artifacts

Based on the above analysis of dating of terrace deposits, it is deduced that the first terrace (T1) formed at ~ 3.5 ka. The second terrace (T2) was dated as ~ 74 ka, while this is slightly older than the ages of the second terrace in the southeastern coastal area of Korean Peninsula^[49,50], the lack of well-dated regional sea level change data impedes further evaluation of the OSL age and its geological implications. The third terrace (T3) was dated to yield an apparent age of ~ 77 ka. For the geomorphologic

evolution of the marine terraces, the third terrace should be older than the second terrace. The OSL age of the third terrace is therefore an underestimated date. If the beach deposits in the region are generally developed during interglacial times, the sediments on the bottom of the T3 would be 125 ka or older. In this case, the Paleolithic artifacts from T3 should be much older than the apparent OSL age of ~77 ka. More dating studies are clearly needed to improve the chronological framework.

3.5 Implication for optical dating of sediments in South China

In optical dating, it is equally important to determine the equivalent dose and the annual dose of a dated sample. It is usually assumed that the annual dose remains constant during burial^[51]. This means that the amount of energy absorbed per year by quartz or feldspar grains from natural radioactivity in the surrounding material should have been constant since burial. In this case, an average annual dose during burial can be calculated by analyzing the contents of radioactive elements.

Quaternary near-surface sediments in South China are readily affected by chemical weathering due to humid tropical and humid subtropical climates. Weathering results in changes in chemical compositions of sediments and redistribution of elements, and causes some elements to migrate and to be relatively enriched in the weathering products. Weathering also affects the structure, fabric, porosity of the sediments^[52]. It is not easy to deduce the timing and the rate of change in chemical compositions of weathered sediments due to difficulty in determining the timing and the rate of weathering. Radionuclide contents determined in the laboratory today do not always represent the average contents during burial. Furthermore, if the weathering causes U-series disequilibrium in weathering products^[53], then the annual dose estimation would be even more complicated. Therefore, it is difficult to determine the average annual dose of weathered sediments during burial. The luminescence ages reported previously for the weathered sediments from South China should be interpreted as underestimated dates or minimal ages if the effect of weathering on annual dose was not properly considered. In dating Quaternary sediments such as “Old Red Sand” from South China, especially for strongly weathered sediments such as laterite, the effect of weathering on

annual dose should be thoroughly investigated. In dating weathered sediments, the best way is to find fresh samples at the bottom of a section which may be unaffected by weathering. If potassium feldspar can be found in weathered sediments, the recently developed potassium feldspar “isochron” methods^{1),[54,55]} can overcome changes in external dose rate, and reliable dates might be obtained. In this case, potassium feldspar isochron age and quartz OSL age of weathered sediments would allow establishment of the timing of weathering and calculation of weathering rate. This would be not only significant for the study of earth surface processes but also useful for environment engineering.

4 Conclusions

Chemical weathering results in changes in chemical composition of the “Old Red Sand” sediment from the coastal areas of South China, which in turn could affect environmental radiation field. Therefore, for weathered sediments such as the “Old Red Sand”, the annual dose calculated from U, Th and K contents which are determined presently in the laboratory cannot represent the average annual dose of a dated sample during burial. In the view of luminescence properties, the “Old Red Sand” sediment is suitable for optical dating, but it is difficult to determine their average annual dose during burial. Nevertheless, the samples from the bottom of “Old Red Sand” sections may be less affected by weathering, so their optical ages are likely to be close to their true burial ages. Alternatively, the potassium feldspar isochron dating methods should be applied to these weathered sediments.

Three marine terraces in the coastal areas of Jinjiang, Fujian Province, China, were identified. The first terrace formed during Holocene. The sediment from the terrace was dated as ~3.5 ka. The “Old Red Sand” sediments, developed in the second and the third terraces, have different degrees of weathering. The age of the “Old Red Sand” sediments from the second terrace is ~74 ka. The sediments and the Paleolithic artifacts from the third terrace are inferred to be older than the apparent OSL age of 77 ka, possibly corresponding to the last or an earlier interglacial.

We thank Dr Gu Zhaoyan for helpful suggestions.

1) Li B, Li S H and Wintle A G. Overcoming environmental dose rate changes in luminescence dating of waterlain deposits. *Geochronometria*, in press.

- 1 Wu Z, Wang W. Formation of “Old Red Sand” and paleogeographic environment on South China coasts. *Sci China Ser D-Earth Sci*, 1998, 41(3): 306—313
- 2 Chen J C, Zeng C S, Wu Y G. Distribution and sedimentary landform of “Old Red Sands” in coastal southeastern Fujian. *J Oceanogr Taiwan Strait* (in Chinese), 1998, 17(1): 50—54
- 3 Jin Z M, Liao B L, Wu Z. Research on laterization of the “Old Red Sand” along the coasts of South China. *Chin Sci Bull*, 1994, 39(12): 1122—1124
- 4 Wu Z, Huang S, Jin Z M, et al. Research on the formation and laterization of the “Old Sandy Sediment” along the coast of South China. *Acta Geogr Sin* (in Chinese), 1994, 49(4): 298—305
- 5 Zeng C S, Chen J C, Wu Y G. A summary of “Old Red Sand” research in coastal southeast China. *J Oceanogr Taiwan Strait* (in Chinese), 1997, 16(3): 367—370
- 6 Zeng C S, Chen J C, Wu Y G. The “Old Red Sand” along the coastal area of southeast Fujian and environmental evolution during Late Quaternary. *J Des Res* (in Chinese), 1999, 19(2): 110—114
- 7 Zeng C S, Chen J C, Wu Y G. Sedimentary stratum and forming age of the “Old Red Sand” along the coast of southeastern Fujian. *J Des Res* (in Chinese), 1999, 19(4): 338-342
- 8 Wu Z, Wang W, Tan H Z, et al. The age of the “old red sand” on the coasts of south Fujian and west Guangdong, China. *Chin Sci Bull*, 2000, 45(13): 1216—1221
- 9 Tan H Z, Wu Z. TL dating of the “Old Red Sand” on the coasts of Fujian and Guangdong. *J Des Res* (in Chinese), 2001, 21(4): 393—396
- 10 Huntley D J, Godfrey-Smith D I and Thewalt M L W. Optical Dating of sediments. *Nature*, 1985, 313: 105—107
- 11 Wintle A G and Huntley D J. Thermoluminescence dating of a deep-sea sediment core. *Nature*, 1979, 279: 710—712
- 12 Aitken M J. *An Introduction to Optical Dating: The Dating of Quaternary Sediments by the Use of Photon-stimulated Luminescence*. Oxford: Oxford University Press, 1998
- 13 Godfrey-Smith D I, Huntly D J and Chen W H. Optical dating studies of quartz and feldspar sediment extracts. *Quat Sci Rev*, 1988, 7: 373—380
- 14 Prescott J R and Robertson G B. Sediment dating by luminescence: a review. *Rad Meas*, 1997, 27: 893—922
- 15 Wintle A G and Murray A S. A review of quartz optically stimulated luminescence characteristics and their relevance in single-aliquot regeneration dating protocols. *Rad Meas*, 2006, 41: 369—391
- 16 Murray A S, Olley J M. Precision and accuracy in the optically stimulated luminescence dating of sedimentary quartz: a status review. *Geochronometria*, 2002, 21: 1—16
- 17 Ballarini M, Wallinga J, Murray A S, et al. Optical dating of young coastal dunes on a decadal time scale. *Quat Sci Rev*, 2003, 22: 1011—1017
- 18 Murray A S, Funder S. Optically stimulated luminescence dating of a Danish Eemian coastal marine deposit: A test of accuracy. *Quat Sci Rev*, 2003, 22: 1177—1183
- 19 Zhang H N, Yao Q Y, Zhao X T. Formation and age of “Old Red Sand” in the coastal areas of south Fujian and east Guangdong. *Mar Geol Quat Geol* (in Chinese), 1985, 5(1): 47—57
- 20 Wu Z, Wang W. Finding and its significance of “Old Red Sand” strata with multiple depositional stages on the coasts of Fujian and Guangdong. *J Des Res* (in Chinese), 2001, 21(4): 328—332
- 21 Xu Q H. Discovery of ancient submerged forest in Shenhuan Bay, Fujian Province, China. *Chin Sci Bull*, 1987, 32(21): 1650—1653
- 22 Xu Q H, Feng Y J, Shi J S. Crustal movement in Shenhuan Bay area, Fujian Province since the middle stage of late pleistocene. *Seismol Geol* (in Chinese), 2002, 24(1): 111—123
- 23 Kim S W. A study on the terraces along the Southeastern coast (Bang-eojin-Pohang) of the Korean peninsula. *J Geol Soc Korea*, 1973, 9: 89—121
- 24 Kim J Y, Lee D Y, Choi S G. A research on Pleistocene stratigraphy. *Korean J Quat Res*, 1998, 4: 41—57
- 25 Prescott J R, Hutton J T. Cosmic ray contributions to dose rates for luminescence and ESR dating: large depths and long-term time variations. *Rad Meas*, 1994, 23: 497—500
- 26 Murray A S, Wintle A G. Luminescence dating of quartz using an improved single-aliquot regenerative-dose protocol. *Rad Meas*, 2000, 32: 57—73
- 27 Bateman M D, Holmes P J, Carr A S, et al. Aeolianite and barrier dune construction spanning the last two glacial-interglacial cycles from the southern Cape coast, South Africa. *Quat Sci Rev*, 2004, 23: 1681—1698
- 28 Gibbertson D D, Schweininger J L, Kemp R A, et al. Sand-drift and soil formation along an exposed north Atlantic coastline: 14,000 years of diverse sedimentological, climatic and human impacts. *J Archaeol Sci*, 1999, 26: 439—469
- 29 Murray A S and Clemmensen L B. Luminescence dating of Holocene aeolian sand movement, Thy, Denmark. *Quat Sci Rev*, 2001, 20: 751—754
- 30 Duller G A T, and Augustinus P C. Reassessment of the record of linear dune activity in Tasmania using optical dating. *Quat Sci Rev* 2006, 25: 2608—2618
- 31 Stokes S, Thomas D S G and Washington R. Multiple episodes of aridity in southern Africa since the last interglacial period. *Nature*, 1997, 388: 154—158
- 32 Faure G. *Principles and Applications of Inorganic Geochemistry*. New York: Macmillan Publ. Co. 1991. 1—626
- 33 Chesworth W. Weathering systems: In: Martini I P, Chesworth W. eds. *Weathering, Soils, and Paleosols*. New York: Elsevier, 1992. 19—40
- 34 Michel J. Redistribution of uranium and thorium series isotopes during isovolumetric weathering of granite. *Geoch Cosm Acta*, 1984, 48: 1249—1255
- 35 Guthrie V A and Kleeman J D. Changing uranium distributions during weathering of granite. *Chem Geol*, 1986, 54: 113—126
- 36 Gueniot B, Munier-Lamy C and Berthelin J. Geochemical behavior of uranium in soils, part I. Distribution of uranium in hydromorphic soils

- and soil sequences. Applications for surficial prospecting. *J Geoch Expl*, 1988, 31: 21–37
- 37 Gueniot B, Munier-Lamy C and Berthelin J. Geochemical behavior of uranium in soils, part II. Distribution of uranium in hydromorphic soils and soil sequences. Applications for surficial prospecting. *J Geoch Expl*, 1988, 31: 39–55
- 38 McAlister J J, Cooney G and Higgins M J. Accumulation of uranium in granitic soils overlying the Mourne Mountains, County Down, northern Ireland. *Microchem J*, 1997, 56: 315–326
- 39 Echevarria G, Sheppard M I, Morel J L. Effect of pH on the sorption of uranium in soils. *J Environ Rad*, 2001, 53: 257–264
- 40 Aubert D, Probst A, Stille P. Distribution and origin of major and trace elements (particularly REE, U and Th) into labile and residual phases in an acid soil profile (Vosges Mountains, France). *Applied Geochem*, 2004, 19: 899–916
- 41 Mibus J, Sachs S, Pflingsten W, Nebelung C, et al. Migration of uranium (IV)/(VI) in the presence of humic acids in quartz sand: A laboratory column study. *J Cont Hydro*, 2007, 89: 199–217
- 42 Peuraniemi V and Aario R. Hydromorphic dispersion of uranium in a surficial environment in northern Finland. *J Geoch Expl*, 1991, 41: 197–212
- 43 Taboada T, Cortizas A M and Garcia C et al. Uranium and thorium in weathering and pedogenetic profiles developed on granitic rocks from NW Spain. *Sci Total Environ*, 2006, 356: 192–206
- 44 Takeda A, Tsukada H and Takaku Y, et al. Accumulation of uranium derived from long-term fertilizer applications in a cultivated Andisol. *Sci Total Environ*, 2006, 367: 924–931
- 45 Osmond J K and Ivanovich M. Uranium-series mobilization and surface hydrology. In: Ivanovich M and Harmon R S, eds. *Uranium-series Disequilibrium*. 2nd ed. Oxford: Clarendon Press, 1992. 260–289
- 46 Gu Z Y, Lal D and Liu T S. Weathering histories of Chinese loess deposits based on uranium and thorium series nuclides and cosmogenic ^{10}Be . *Geoch Cosm Acta*, 1997, 61: 5221–5231
- 47 Zhang J F, Zhou L P and Yue S Y. Dating fluvial sediments by optically stimulated luminescence: selection of equivalent doses for age calculation. *Quat Sci Rev*, 2003, 22: 1123–1129
- 48 Pei S W, Zhang J F, Gao X, et al.. Optical dating of the Jingshuiwan Paleolithic site of Three Gorges, China. *Chin Sci Bull*, 2006, 51(11): 1334–1342
- 49 Choi J H, Murray A S, Jain M, et al. Luminescence dating of well-sorted marine terrace sediments on the southeastern coast of Korea. *Quat Sci Rev*, 2003, 22: 407–421
- 50 Choi J H, Murray A S, Cheong C S, et al. The resolution of stratigraphic inconsistency in the luminescence ages of marine terrace sediments from Korea. *Quat Sci Rev*, 2003, 22: 1201–1206
- 51 Aitken M J. *Thermoluminescence Dating*. London: Academic Press, 1985
- 52 Jeong G Y, Cheong C S and Choi J H. The effect of weathering on optically stimulated luminescence dating. *Quat Geochronol*, 2007, 2: 117–122
- 53 Chabaux F, Dequincey O, Leveque J J, et al. Tracing and dating recent chemical transfers in weathering profiles by trace-element geochemistry and ^{238}U - ^{234}U - ^{230}Th disequilibria: the example of the Kaya lateritic toposequence (Burkina-Faso). *Comp Rend Geosci*, 2003, 335: 1219–1231
- 54 Zhao H and Li S H. Luminescence isochron dating: a new approach using different grain sizes. *Rad Prot Dos*, 2002, 101: 333–338
- 55 Zhang J F. Development and application of luminescence dating to Quaternary sediments from China. Dissertation for the Doctoral Degree. Hong Kong: Hong Kong University, 2000